Programmable filterless network architecture based on optical white boxes

Marija Furdek*, Ajmal Muhammad*, Georgios Zervas†, Nabih Alloune‡, Christine Tremblay‡ and Lena Wosinska*
*School of ICT, KTH Royal Institute of Technology, Kista, Sweden
Email: marifur@kth.se
†High-performance Networks Group, University of Bristol, United Kingdom
‡Department of Electrical Engineering, École de technologie supérieure, Montréal, Canada

***Abstract*—We propose and evaluate a novel architecture enabling high-capacity, resource efficient and agile elastic optical networks. It is based on sliceable bandwidth-variable transponders and optical white box switches which route optical signals without filtering them. Instead of using active filtering components, each node is equipped with an optical white box based on a programmable optical switch that serves as an optical backplane. It provides interconnections between input/output ports and passive splitters and couplers. Due to signal broadcast and the absence of filtering (so-called *drop-and-waste* transmission), some of the signals appear on unintended links which can lead to an overhead in spectrum usage. To address this issue, we formulate the problem of signal routing, modulation format and spectrum assignment in programmable filterless networks based on optical white boxes as an integer linear program (ILP) with the objective to minimize the total spectrum usage. Simulation results indicate that our proposed solution obtains a beneficial tradeoff between component usage and spectrum consumption, using a drastically lower number of active switching elements than the conventional networks based on hard-wired reconfigurable add/drop multiplexers, and lowering the maximum used frequency slot by up to 48% compared to existing passive filterless networks.**

***Index Terms*—Filterless optical networks; coherent elastic transmission; optical white box; wavelength routing; mathematical programming.**

I. Introduction

Optical networking has been recognized as the only viable technology to support the long-term growth of network traffic. As new network applications with diverse and time-varying bit rate requirements emerge, optical networking faces the need to provide high-capacity, cost-efficient and agile solutions which support elastic and flexible spectrum usage and offer high reliability performance. Recent advances in coherent transmission with digital signal processing enable the new generation of high-capacity optical networking. The standard ITU spectrum division into fixed grid with 50 GHz channel spacing is giving way to the elastic, flexible grid networking with finer spectrum granularity where channels are created of multiple frequency slot units (FSUs) (e.g., 12.5 GHz) and with flexible central frequencies. A new generation of sliceable bandwidth variable transponders (S-BVTs) enables formation of super-channels, where multiple adjacent subcarriers compose a single optical connection [1]. They also support sliceability, where a number of subcarriers from a single transmitter can be grouped to form super-channels directed towards different destinations.

Optical switches are considered as another key element for enabling conventional elastic, transparent optical networks. Currently, the majority of reconfigurable optical add/drop multiplexers (ROADMs) employs a hard-wired architecture where the interconnections between nodal components (e.g., spectrum selective switches (SSSs)) cannot be changed without manual intervention. The optical white boxes (also referred to as Architecture on Demand or synthetic, programmable switches) were recently proposed as a promising alternative to conventional, hard-wired ROADMs [2]. In an optical white box, optical modules, such as splitters, amplifiers, or SSSs are interconnected through a programmable optical backplane (i.e., optical space switch, e.g., [3]) in contrast to the conventional ROADMs. Inside a white box, connections use only the components needed to satisfy the processing requirements and bypass unneeded components, which improves cost, resource usage and reliability performance. Moreover, the use of active backplane switch allows for ease of migration, seamless capacity scaling, and deployment of different function blocks (network or compute) where and when needed for applications such as 5G and Fog Computing.

The advances in elastic coherent transmission allow for simplifications in the network architecture, by, for example, enabling colorless ROADM architecture where costly add/drop wavelength switches are replaced by passive splitters and couplers [4]. The passive filterless network architecture has further extended this concept to completely eliminate the need for active switching components even for transit traffic [5]. Passive filterless networks based on elastic coherent transmission have been proposed as a promising concept enabling agile, flexible solutions for both terrestrial and submarine applications. Their architecture is based on optical fiber links interconnected by passive optical couplers and splitters, forming a passive fiber-tree topology between nodes. Agility of passive filterless networks is achieved by tuning the transmitters and receivers at the edge nodes. The express function at the intermediate nodes is realized in a completely passive manner, eliminating the need for any filtering and inherently supporting flexgrid operation. Due to the absence of active switching components, passive filterless networks are characterized by low initial deployment cost, as well as high reliability performance stemming from lower failure rates of passive components.

The transmission in passive filterless networks follows the so-called *drop-and-waste* (or *drop-and-continue*) principle, which gives rise to certain disadvantages. Due to the absence of filtering, signals continue to propagate along the fiber tree beyond the destination node. Moreover, the signal from each transmitter is broadcasted to all branches of the corresponding fiber tree downstream of the source node. The spectrum used by these unfiltered signals on unintended branches cannot be reused by any co-propagating channels, which can lead to a waste of spectrum. Broadcasting signals to inadvertent nodes other than the targeted destination(s) raises privacy issues. Additional concerns stem from the fiber tree topology which needs to be pre-planned so as to satisfy the reach constraints on all demands, and cannot be flexibly reconfigured.

To address the drawbacks of passive filterless networks and combine their advantages with the flexibility offered by programmable switches, we propose a novel, programmable optical network architecture based on filterless operation supported by optical white boxes. We quantify the potential benefits of our proposed solution w.r.t. resource usage by formulating the routing, modulation format and spectrum assignment (RMSA) problem as an integer linear program (ILP) with the objective to minimize spectrum consumption and compare the obtained solutions to the passive filterless and conventional filtered network architecture.

The remainder of the paper is organized as follows. Section II provides an overview of the state of the art in the related technologies. Section III introduces the principles of the proposed programmable filterless white box networking and illustrates them on a simple example. Section IV defines the RMSA problem in programmable filterless networks and presents the corresponding ILP formulation. Section V analyzes the performance of the approach by comparison with benchmarking solutions, and Section VI concludes the paper.

II. State of the Art

A. Passive Filterless Networking

A detailed description of the concept of filterless networking, the supporting network architecture and the definition of the filterless network design problem can be found in [5]. The authors therein also demonstrate significant savings in terms of device costs of passive filterless networks compared to conventional filtered solutions due to the absence of active switching components, coming at a trade-off with increased spectrum usage of about 25%. A validation of the physical layer performance of passive filterless networks was carried out in [6], while a control plane solution based on path computation element (PCE) was presented in [7]. The dynamic operation of filterless network supported by the proposed control plane was evaluated in [8], indicating similar trends in the resource usage overhead as in the static scenario [5]. Resilience issues were addressed in [9] by constructing the optical fiber trees so as to guarantee for at least two link-disjoint paths between each pair of nodes in the network.

While the aforementioned work refers to the fixed-grid scenario based on the standard fixed ITU frequency grid with 50 GHz channel spacing, passive filterless networks represent a very suitable solution for elastic optical networking. An overview of elastic core optical networking was presented in [10]. Numerous approaches based on ILP formulation and heuristic algorithms for solving the routing and spectrum assignment (RSA) problem in conventional, filtered elastic networks can be found in, e.g., [11], [12] and the references therein. However, standard RSA approaches cannot be directly applied in passive filterless networks as they do not account for the unfiltered channels which are due to the signal branching and the drop-and-waste transmission.

Elastic passive filterless networks were recently introduced in [13], along with a heuristic approach for survivable RSA with dedicated path protection. The RSA problem with the objective of minimizing spectrum usage in passive filterless networks (unprotected design) was further studied in [14]. Therein, ILP-based and heuristic approaches were proposed for larger network instances, obtaining between 35% and 56% lower spectrum usage than when fixed grid is deployed. An experimental evaluation of vendor-interoperable interfaces supported by the filterless networks was performed in [15]. Preliminary trial deployments in pilot networks based on passive filterless operation were carried out in Croatia (2012) and Germany (2014) [16].

B. Optical White Boxes

Optical white boxes were proposed recently as a technological solution allowing for unprecedented flexibility in nodal architecture design and network provisioning [2]. An overview of different types of flexibility enabled by this technology (i.e., switching, routing and architectural flexibility) can be found in [2], along with the experimental demonstration of their feasibility and benefits. Procedures for synthesis of the nodal architecture in order to support a given traffic mapping between input and output ports of the node can be found in [17]. The related analysis of scalability, power consumption and cost indicated that, due to aggregation of channels into fiber-switched port pairs, white boxes allow for a decrease in the number of used optical backplane ports and the resulting cost and power consumption.

Cost-efficient network planning approaches for white box-based elastic networks considering static and dynamic traffic scenarios were proposed in [18]. Their common objective is to dimension network nodes and perform routing and spectrum assignment to connection requests in a way which minimizes the number of used components. The impact of white box deployment to the availability of connections in the network was evaluated in [19], showing strong reduction in network downtime. Note that in all of these studies, optical white boxes were used to create complex ROADM structures, where the optical backplane interconnects other active components such as SSSs, amplifiers, or sub-wavelength switches. However, in this paper we assume that the optical backplane supports fiber switching and uses only passive components to split or couple signals between different ports when fiber switching is not feasible.

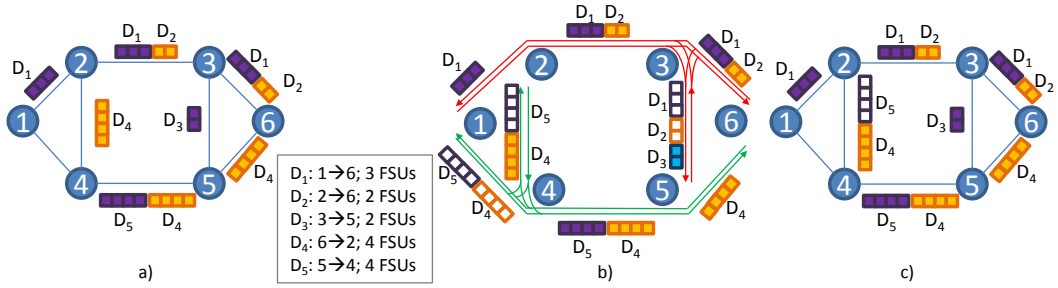

Figure 1. An illustrative example: a 6-node network topology and five unidirectional demands ($D_1 - D_5$), and solutions deploying a) conventional ROADMs, b) passive filterless network, and c) programmable filterless network architecture.

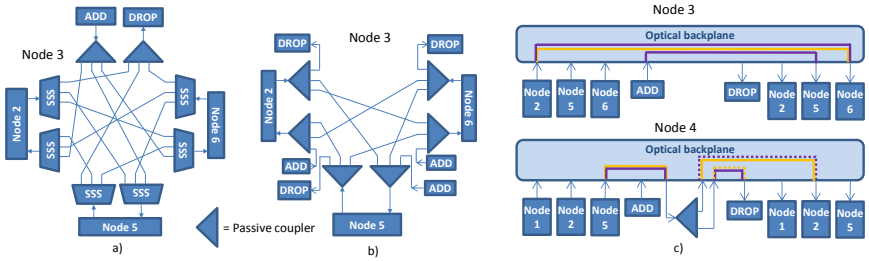

Figure 2. Detailed node setup supporting the example from Fig. 1: a) Node 3 in the conventional ROADM network, b) Node 3 in the passive filterless network, c) Node 3 and Node 4 in the white box-based programmable filterless network architecture.

III. Programmable Filterless Networks Based on Optical White Boxes

In programmable filterless white box networks, interconnections between nodes are formed with the help of programmable switches that serve as optical backplane. Inside each node, express function is realized by either fiber switching, i.e., directly connecting a pair of input and output ports and bypassing all components in the node, or by interconnecting the necessary ports via passive splitters and couplers. This allows for greater flexibility in routing and reduces the broadcasting of signals to unintended ports, which in turn decreases spectrum waste and enhances privacy compared to the passive filterless solution. Note that the optical switch is used as a space switch to support the necessary interconnections between ports, and no filtering elements are applied. Compared to filtered solutions based on conventional ROADMs which deploy a number of SSSs per node, this can bring significant savings in cost and inherent support of gridless operation.

A. An Illustrative Example

Fig. 1 shows a simple illustrative example of the proposed programmable filterless network architecture. In the example, a 6-node physical topology and five communication demands (denoted as $D_1 - D_5$) are given. A feasible solution based on conventional ROADMs is shown in Fig. 1 a). One possible solution accommodating the demands using a passive filterless network is shown in Fig. 1 b). The depicted passive solution is based on two fiber trees, shown in red and green, respectively. Demands $D_1 - D_3$ are routed over the red tree, while D_4 and D_5 use the green tree. The filled slots represent the useful signals, while the empty ones denote the unfiltered signals present due to the signal broadcast and drop-and-waste transmission. Fig. 1 c) shows a possible solution deploying programmable filterless architecture. Compared to Fig. 1 b), the white box-based network has a lower spectrum waste caused by unfiltered channels, implying a greater possibility of spectrum reuse (see, e.g., D_3 on link $3-5$), and enhanced privacy (see how, e.g., in the white box-based solution only D_5 propagates to one unintended node (Node 2), whereas in the passive solution D_5 is received by Nodes 1 and 2, while D_1 and D_2 propagate to Node 5).

Fig. 2 depicts details of the architecture of representative nodes supporting the three solutions. Fig. 2 a) shows a conventional ROADM with *route-and-select* configuration deployed in Node 3 of the example network. In general, a node with degree d will require $2d$ SSSs to support the express traffic in this configuration, plus a splitter and a coupler in the add/drop part. Fig. 2 b) depicts the architecture of Node 3 in the passive filterless solution, comprising 8 1:3 splitters. In general, a node with degree d will require $2d$ 1:d splitters to support this configuration. The actual splitting ratio undergone by signals can be higher, determined by the commercially available splitters (e.g., 1:2, 1:4, 1:8, etc.). For the white box-based solution, the architecture of Nodes 3 and 4 is depicted in Fig. 2 c). In general, each node uses a single optical $N \times N$ switch whose size depends on the degree of the node and on the number and degree of the necessary passive devices. As shown for Node 3, the support of fiber switching allows for signals to be forwarded directly from an input to an output port, bypassing unnecessary components. Thus, D_1 and D_2

are sent from the incoming port from Node 2 to the outgoing port towards Node 6, while D_3 is added towards Node 5. A scenario where fiber switching is not possible is shown for Node 4 in Fig. 2 c). There, signals on D_4 and D_5 are not intended to the same output port so they must be split before being directed to their corresponding outputs. Due to the absence of filtering, parts of each signal remain present on both split copies (represented by dashed lines). However, compared to the passive solution, a lower number of splitters/couplers is used and their degree is lower. Combined with fiber switching, this translates to a lower insertion loss and a lower number of used ports of the optical switching backplane.

IV. Routing, Modulation Format and Spectrum Assignment in Programmable Filterless Networks

A. Problem Definition

In this paper, we solve the routing, modulation format and spectrum assignment (RMSA) problem in programmable filterless networks based on white boxes with the objective to minimize spectrum usage. The problem can be formally defined as follows. Given a physical topology represented by a graph $G(V, E)$ comprising a set of nodes V and a set of links E, and a set of traffic demands D, we must find a physical route through the network, select a modulation format and assign the appropriate number of spectrum slots to each demand. Due to the presence of unfiltered signals, the RMSA problem in filterless networks differs from its counterpart in conventional, filtered networks. Additionally, in white box-based networks, the solution of the RMSA problem and the nodal architecture, i.e., the type and number of used components and their interconnections via the optical backplane, are interdependent. When solving the RMSA problem, the spectrum continuity and contiguity constraints must hold, implying that the spectrum slots used by a demand must be the same along all links included in the path, they must be adjacent, and there can be no spectrum overlapping among different channels.

B. ILP Formulation of the RMSA Problem

Input parameters

- $\mathcal{G}(\mathcal{V}, \mathcal{E})$: a directed graph where $\mathcal{V}$ is the set of vertices that represent the network nodes, $\mathcal{E}$ is the set of arcs that represent the network links;
- L: set of available line rates with matching modulation format M, spectrum width B, and reach R, respectively;
- D: set of traffic demands, where each element d defines the number of requested spectrum slots T_d from source node $s_d \in \mathcal{V}$ to destination node $t_d \in \mathcal{V}$ according to the line rate selection method;
- P: set of physical routes, where each element P_d defines a set of candidate physical routes for demand $d \in \mathsf{D}$;
- $\mathsf{K} = \{K_1, K_2, ..., K_{|\cup P_d \in \mathsf{P}|}\}$: set of constants with distinct values used for assigning a unique identifier to each path in P;
- $\tau_{p^d, p^{\hat{d}}}$: indicator for disjoint routes, equal to 0 when $p^d \in P_d$ and $p^{\hat{d}} \in P_{\hat{d}}$ are link disjoint, and 1 otherwise;
- $\Gamma_{p^d, p^{\hat{d}}}$: set of links $\in p^{\hat{d}}$ unintentionally traversed by the established optical channel for d over path p^d due to the broadcasting nature of the optical splitter;
- C: large constant;

Variables

- $x_{p^d} \in \{0, 1\}$ - equal to 1 if path $p^d \in P_d$ is used by $d \in \mathsf{D}$ and 0 otherwise;
- $s_{p^d} \in \{0, 1\}$ - equal to 1 if spectrum slots T_{p^d} on path p^d are used by d and 0 otherwise;
- $f_d \in \mathbb{Z}^+$ - the starting spectrum slot number for d;
- $\Psi^{(d,\hat{d})}_{p^d, p^{\hat{d}}} \in \{0, 1\}$ - equal to 1 if p^d and $p^{\hat{d}}$ are used by demands d and $\hat{d}$, respectively, and 0 otherwise;
- $\Upsilon^{(d,\hat{d})}_{p^d, p^{\hat{d}}} \in \mathbb{Z}^+$ - the number of unintended links traversed by d when p^d and $p^{\hat{d}}$ are used by demands d and $\hat{d}$, resp.;
- $\delta^{(d,\hat{d})} \in \{0, 1\}$ - equal to 0 if the starting slot number of d is greater than $\hat{d}$ (i.e., $f_d > f_{\hat{d}}$) and 1 otherwise;
- $\delta^{(\hat{d},d)} \in \{0, 1\}$ - equal to 0 if the starting slot number of $\hat{d}$ is greater than d (i.e., $f_{\hat{d}} > f_d$) and 1 otherwise;
- $\mathsf{M_s}$ - the maximum allocated spectrum slot number among all network links;

Objective function

$$Minimize : \mathsf{M_s} \tag{1}$$

Constraints

$$\sum_{p^d \in P_d} x_{p^d} = 1 \quad \forall d \in \mathsf{D} \tag{2}$$

$$f_d + \sum_{p^d \in P_d} T_{p^d} \cdot s_{p^d} - 1 \leq \mathsf{M_s} \quad \forall d \in \mathsf{D} \tag{3}$$

$$K_{p^d} \cdot x_{p^d} - K_{p^d} \cdot s_{p^d} = 0 \quad \forall d \in \mathsf{D}, \forall p^d \in P_d \tag{4}$$

$$\begin{gathered} x_{p^d} + x_{p^{\hat{d}}} - \mathsf{C} \cdot \Psi^{(d,\hat{d})}_{p^d, p^{\hat{d}}} \leq 1 \\ \forall (d, \hat{d}) \in \mathsf{D}, \forall p^d \in P_d, \forall p^{\hat{d}} \in P_{\hat{d}} \end{gathered} \tag{5}$$

$$\begin{gathered} \Upsilon^{(d,\hat{d})}_{p^d, p^{\hat{d}}} - |\Gamma_{p^d, p^{\hat{d}}}| \cdot \Psi^{(d,\hat{d})}_{p^d, p^{\hat{d}}} = 0 \\ \forall (d, \hat{d}) \in \mathsf{D}, \forall p^d \in P_d, \forall p^{\hat{d}} \in P_{\hat{d}} \end{gathered} \tag{6}$$

$$\begin{gathered} \Psi^{(d,\hat{d})}_{p^d, p^{\hat{d}}} + \tau_{p^d, p^{\hat{d}}} - 1 \leq 2 \cdot \delta^{(d,\hat{d})} + 2 \cdot \delta^{(\hat{d},d)} \\ \forall (d, \hat{d}) \in \mathsf{D}, \forall p^d \in P_d, \forall p^{\hat{d}} \in P_{\hat{d}} \end{gathered} \tag{7}$$

$$\begin{gathered} f_d - f_{\hat{d}} + \mathsf{C} \cdot (\delta^{(d,\hat{d})} + x_{p^d} + x_{p^{\hat{d}}}) \leq 3 \cdot \mathsf{C} - T_{p^d} \\ \forall (d, \hat{d}) \in \mathsf{D}, \forall p^d \in P_d, \forall p^{\hat{d}} \in P_{\hat{d}} \end{gathered} \tag{8}$$

$$\begin{gathered} f_{\hat{d}} - f_d + \mathsf{C} \cdot (\delta^{(\hat{d},d)} + x_{p^d} + x_{p^{\hat{d}}}) \leq 3 \cdot \mathsf{C} - T_{p^{\hat{d}}} \\ \forall (d, \hat{d}) \in \mathsf{D}, \forall p^d \in P_d, \forall p^{\hat{d}} \in P_{\hat{d}} \end{gathered} \tag{9}$$

$$\begin{gathered} \Psi^{(d,\hat{d})}_{p^d, p^{\hat{d}}} + x_{p^{\tilde{d}}} \leq \delta^{(d,\tilde{d})} + \delta^{(\tilde{d},d)} + 1 \\ \forall (d, \tilde{d}) \in \mathsf{D} : \Gamma_{p^d, p^{\hat{d}}} \cap p^{\tilde{d}} \neq \{\emptyset\}, \forall p^d \in P_d, \forall p^{\tilde{d}} \in P_{\tilde{d}} \end{gathered} \tag{10}$$

$$f_d - f_{\tilde{d}} + \mathsf{C}\cdot(\delta^{(d,\tilde{d})} + \Psi^{(d,\hat{d})}_{p^d,p^{\hat{d}}} + x_{p^{\tilde{d}}}) \leq 3\cdot\mathsf{C} - T_{p^{\tilde{d}}} \quad (11)$$
$$\forall(d,\tilde{d}) \in \mathsf{D} : \Gamma_{p^d,p^{\hat{d}}} \cap p^{\tilde{d}} \neq \{\emptyset\}, \forall p^d \in P_d, \forall p^{\tilde{d}} \in P_{\tilde{d}}$$

$$f_{\tilde{d}} - f_d + \mathsf{C}\cdot(\delta^{(\tilde{d},d)} + \Psi^{(d,\hat{d})}_{p^d,p^{\hat{d}}} + x_{p^{\tilde{d}}}) \leq 3\cdot\mathsf{C} - T_{p^{\tilde{d}}} \quad (12)$$
$$\forall(d,\tilde{d}) \in \mathsf{D} : \Gamma_{p^d,p^{\hat{d}}} \cap p^{\tilde{d}} \neq \{\emptyset\}, \forall p^d \in P_d, \forall p^{\tilde{d}} \in P_{\tilde{d}}$$

The objective (1) is to minimize the maximum utilized spectrum slot ($\mathsf{M_s}$) among all network links. Constraint (2) guarantees that a single route is assigned to each d. Constraint (3) assigns a contiguous set of spectrum slots to d. Constraint (4) makes sure that the selected spectrum resources are available along the chosen route. Constraints (5,6) identify the links over which optical channels propagate unintentionally, due to the drop-and-waste property. Constraints (7-9) ensure the spectrum continuity constraint and non-overlapping spectrum allocation to different traffic demands that utilize routes with common link(s). Similarly, constraints (10-12) make sure that the spectrum slots occupied by the optical channels on the unintended links are not assigned to any other demand $\tilde{d}$.

V. Numerical Results

To evaluate the performance of the proposed programmable filterless network architecture, we solve the ILP formulation and compare the obtained results against two benchmarking solutions based on *(i)* passive filterless and *(ii)* conventional ROADMs. For scalability reasons, we solve the ILP for two smaller networks, shown in Fig. 3.

Fig. 4 shows the detailed setup of the white boxes in each node of the 6-node network (Fig. 3 a)) for random traffic. As can be seen from the figure, each node comprises one programmable optical backplane and optionally passive components (depicted with smaller black rectangles). The interconnections between input/output ports and passive couplers (20 in total) are shown with dashed lines.

Fig. 5 shows the spectrum usage for the 6-node network with uniform and random traffic. The uniform traffic matrix consists of 10 Gbit/s demands between each node pair. The random traffic matrix comprises randomly generated traffic demands of up to 400 Gbit/s per node pair. The ILP formulation used to obtain solutions for the passive filterless network, and the detailed results can be found in [14]. Results for the conventional ROADM-based network were obtained by modifying the ILP formulation presented in Section IV.B so as to drop the signal broadcast and drop-and-continue transmission. As supported by the figure, the white box-based filterless network reduces spectrum usage by 14.5% with respect to the passive filterless solution, averaged over the two scenarios. The

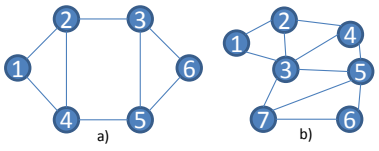

Figure 3. The a) 6-node and b) 7-node German network topology used for simulations.

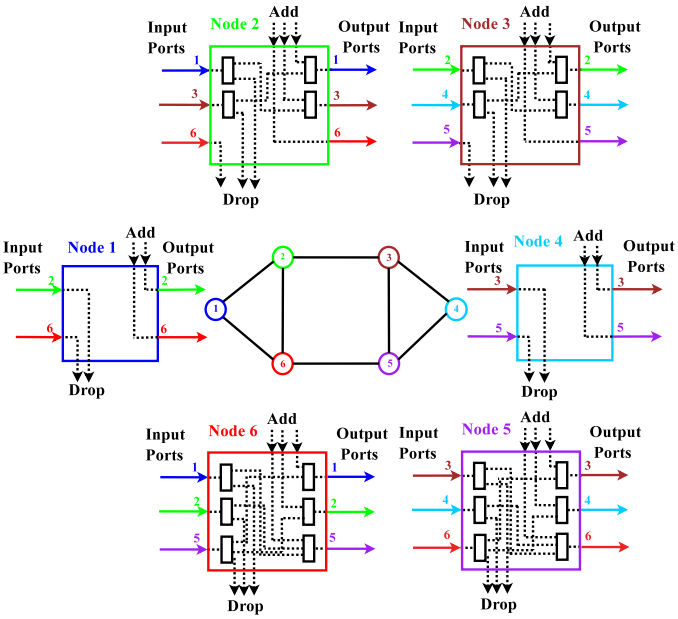

Figure 4. Programmable filterless network architecture obtained by solving the ILP for the random traffic scenario in the 6-node network.

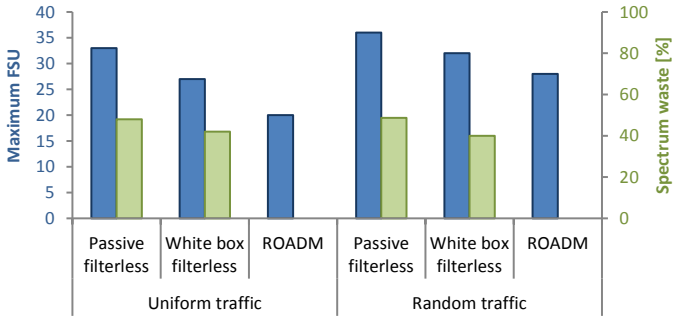

Figure 5. Spectrum usage for the 6-node network test cases.

secondary y-axis shows the percentage of spectrum occupied by unfiltered channels. For the white box filterless network, spectrum waste is on average 15-20% smaller than for the passive filterless. On average, the programmable filterless network requires 22.9% more spectrum than the conventional ROADM case. However, this tradeoff seems reasonable when we consider component usage and the related cost. A detailed breakdown of the types and sizes of necessary components is shown in Table I. In the programmable filterless architecture, each connection traverses on average 2.76 and 2.2 passive couplers for the uniform and random traffic case, respectively. For the passive filterless architecture, these respective values equal 3.14 and 3.71. The average hop count in white box (passive) filterless networks is 1.8 and 1.53 (1.57 and 1.71) for the uniform and random traffic, respectively. From the above, it follows that connections in the programmable filterless network architecture traverse on average 1.53 and 1.44 couplers per hop for the two respective traffic patterns, while these values for passive filterless equal 2 and 2.17. The

Table I
COMPONENT USAGE FOR THE 6-NODE PROGRAMMABLE FILTERLESS NETWORK ARCHITECTURE.

Node	Required switch size		Number of couplers		Maximum coupler degree	
	Uniform	Random	Uniform	Random	Uniform	Random
1	4x4	7x7	0 (0)	2 (0)	- (-)	1:2 (-)
2	12x12	14x14	4 (6)	5 (6)	1:2 (1:3)	1:3 (1:3)
3	12x12	14x14	4 (6)	5 (6)	1:2 (1:3)	1:3 (1:3)
4	4x4	7x7	0 (0)	2 (0)	- (-)	1:2 (-)
5	16x16	14x14	6 (1)	5 (1)	1:3 (1:2)	1:3 (1:2)
6	16x16	14x14	6 (1)	5 (1)	1:3 (1:2)	1:3 (1:2)

Numbers in brackets refer to passive filterless architecture.

Table II
COMPONENT USAGE FOR THE 7-NODE PROGRAMMABLE FILTERLESS NETWORK ARCHITECTURE.

Node	Required switch size	Number of couplers	Maximum coupler degree
1	4x4	0 (0)	- (-)
2	12x12	4 (4)	1:2 (1:2)
3	18x18	6 (8)	1:3 (1:4)
4	12x12	4 (6)	1:2 (1:3)
5	23x23	8 (6)	1:3 (1:3)
6	4x4	0 (0)	- (-)
7	10x10	3 (4)	1:2 (1:2)

Numbers in brackets refer to passive filterless architecture.

lower number of traversed couplers and the lower hop count in the programmable filterless architecture may compensate for the end-to-end insertion loss of the optical backplane switches (about 1 dB per cross-connection, i.e. maximum 3dB per node). Moreover, the fiber switching in some nodes may decrease the number of necessary amplifiers.

To evaluate the performance of our approach on a more realistic network instance, we use the 7-node German network topology from Fig. 3 b) and a realistic traffic matrix from [14] with a total traffic load of 5.4 Tbit/s. Due to scalability issues, the results for the passive filterless architecture were obtained using an evolutionary heuristic from [14]. The maximum FSU used in the white box-based filterless case is 26, while for the passive filterless and conventional ROADM case it takes the values of 50 and 20, respectively, indicating a 48% savings in spectrum usage compared to the passive solution. The wasted spectrum in the white box network architecture equals 39%, which is an additional improvement from the 45% waste in the passive filterless network.

Table II shows the characteristics of the used components. Here, the reduction in the degree and the number of couplers in the programmable filterless compared to the passive filterless architecture is more distinct than for the 6-node network, which can be explained by the higher average nodal degree (3.14 vs. 2.67) and greater flexibility in route selection. Moreover, compared to a conventional ROADM-based solution, programmable filterless architecture requires a single optical switch per node, which is significantly lower than the cost of a flexgrid-enabled ROADM.

VI. CONCLUSION

We propose programmable filterless network architecture based on coherent elastic transmission and optical white box switches. We formulate the routing, modulation format and spectrum assignment problem in these networks as an integer linear program with the objective of minimizing spectrum usage and compare the obtained solutions with passive filterless and conventional ROADM-based networks. Preliminary results indicate that the proposed programmable filterless architecture has the potential to obtain agile, flexible solutions at a significantly lower cost than conventional ROADM-based networks, while using up to 48% lower maximum FSU than passive filterless solutions and reducing the spectrum waste inherent to the *drop-and-waste* filterless transmission.

REFERENCES

[1] N. Sambo *et al.*, "Next generation sliceable bandwidth variable transponders," *IEEE Commun. Mag.*, vol. 53, no. 2, pp. 163-171, Feb. 2015.

[2] N. Amaya, G. Zervas, D. Simeonidou, "Introducing node architecture flexibility for elastic optical networks," *IEEE/OSA J. Opt. Commun. Netw.*, vol. 5, no. 6, pp. 593-608, Jun. 2013.

[3] Polatis Series 6000n Network Optical Switch [Online]. Available: http://www.polatis.com/datasheets/products/Polatis-192x192-6000n-Network-Optical-Switch.pdf, 2016.

[4] B. Zhang, C. Malouin, T. J. Schmidt, "Towards full band colorless reception with coherent balanced receivers," *Opt. Express*, vol. 20, no. 9, pp. 10339-10352, Apr. 2012.

[5] É. Archambault *et al.*, "Design and simulation of filterless optical networks: problem definition and performance evaluation," *IEEE/OSA J. Opt. Commun. Netw.*, vol. 2, no. 8, pp. 496-501, Aug. 2010.

[6] J. P. Savoie, C. Tremblay, D. V. Plant, and M. P. Bélanger, "Physical layer validation of filterless optical networks," in Proc. *ECOC*, 2010.

[7] G. Mantelet *et al.*, "PCE-based centralized control plane for filterless networks," *IEEE Commun. Mag.*, vol. 51, no. 1, pp. 44-51, Jan. 2014.

[8] G. Mantelet *et al.*, "Establishment of dynamic lightpaths in filterless optical networks," *IEEE/OSA J. Opt. Commun. Netw.*, vol. 5, no. 9, pp. 1057-1065, Sep. 2013.

[9] Z. Xu *et al.*, "1+1 dedicated optical-layer protection strategy for filterless optical networks," *IEEE Commun. Lett.*, 18(1), pp. 98-101, Jan. 2014.

[10] G. Zhang *et al.*, "A survey on OFDM-based elastic core optical networking," *IEEE Commun. Surv. Tut.*, vol. 15, no. 1, pp. 65-87, Jan. 2013.

[11] A.N. Patel *et al.*, "Routing, wavelength assignment, and spectrum allocation algorithms in transparent flexible optical WDM networks," *Opt. Switching and Netw.*, vol. 9, no. 3, pp. 191-204, Feb. 2012.

[12] M. Tornatore *et al.*, "On the complexity of routing and spectrum assignment in flexible-grid ring networks [Invited]," *IEEE/OSA J. Opt. Commun. Netw.*, vol. 7, no. 2, pp. A256-A267, Feb 2015.

[13] Z. Xu *et al.*, "Flexible wavelength assignment in filterless optical networks," *IEEE Commun. Lett.*, vol. 19, no. 4, pp. 565-568, Apr. 2015.

[14] É. Archambault *et al.*, "Routing and spectrum assignment in elastic filterless optical networks," to appear in *IEEE/ACM T. Network*.

[15] M. Gunkel *et al.*, "Vendor-interoperable elastic optical interfaces: Standards, experiments, and challenges [Invited]," *IEEE/OSA J. Opt. Commun. Netw.*, vol. 7, no. 12, pp. B184-B193, Dec. 2015.

[16] A. Clauberg, "IPv6 deployment in Germany and Croatia," [Online]. Available: http://www.ipv6observatory.eu/wp-content/uploads/2012/11/01-06-Axel-Clauber1.pdf.

[17] M. Garrich *et al.*, "Architecture on Demand design for high-capacity optical SDM/TDM/FDM switching," *IEEE/OSA J. Opt. Commun. Netw.*, vol. 7, no. 1, pp. 21-35, Jan. 2015.

[18] A. Muhammad *et al.*, "Introducing flexible and synthetic optical networking: Planning and operation based on network function programmable ROADMs," *IEEE/OSA J. Opt. Commun. Netw.*, vol. 6, no. 7, pp. 635-648, Jul. 2014.

[19] M. Džanko *et al.*, "Evaluating availability of optical networks based on self-healing network function programmable ROADMs," *IEEE/OSA J. Opt. Commun. Netw.*, vol. 6, no. 11, pp. 974-987, Nov. 2014.